

## INTRACAVITY FLUX DEPENDENT ABSORPTION IN E-BEAM PUMPED KrF

J.F. Seamans, W.D. Kimura  
Spectra Technology, Inc.  
2755 Northup Way  
Bellevue, Washington 98004-1495

and

D.E. Hanson  
Los Alamos National Laboratory  
P.O. Box 1663, MS-J589  
Los Alamos, New Mexico 87545

Abstract

Transient absorption measurements are performed on e-beam excited KrF under lasing and nonlasing conditions for 10% Kr (Ar diluent) and 99.8% Kr gas mixtures. The intracavity flux is varied by changing the output mirror reflectivity. The deposition rate for this experiment is  $\approx 388 \text{ kW/cm}^3$ . For the 10% Kr and Kr-rich mixtures, the small signal absorption at 248.4 nm is 0.76%/cm and 1.25%/cm, respectively; while the nonsaturable absorption is 0.62%/cm and 0.90%/cm, respectively. A flux loading of  $\approx 1.5 \text{ MW/cm}^2$  is needed to achieve nearly complete saturation of the saturable absorption.

Background

In an ongoing effort to support the KrF laser modeling program at Los Alamos National Laboratory (LANL), Spectra Technology, Inc. (STI) has been conducting various experiments on its e-beam pumped laser facility (Tahoma). One of the goals of these experiments is to generate a complete set of data at a known operating condition in order to provide data to help validate the LANL model. The Tahoma laser facility has proved to be a device very suitable for such a task. The laser has been used extensively in many experiments. It is both a well characterized and reliable device. Some of the experiments included in the set of KrF characterization data are transient absorption and gain measurements under lasing (loaded) and nonlasing (unloaded) conditions, e-beam pumping characterization measurements, and intrinsic efficiency measurements. This paper discusses the transient absorption experiment results.

Description of Experiment

The laser is a Marx powered cold-cathode vacuum diode that delivers  $\approx 375 \text{ keV}$  electrons at the foil. A magnetic guide field of 2 kgauss confines the e-beam to a 6 cm x 70 cm area at an average current density of  $\approx 32 \text{ A/cm}^2$ . The pulse length is variable, but for this work it is  $\approx 450 \text{ ns}$ . The cylindrical active volume of 3.5 cm dia. x 70 cm is located 3.5 cm away from the e-beam foil.

Absorption in the laser active volume is obtained by measuring the input and output intensities of a tunable pulsed probe laser passing twice through the laser chamber. Measurements are made during lasing and nonlasing conditions in order to investigate the dependence of the absorption on the laser flux. A similar technique has been used by others<sup>1,2</sup> to measure the absorption characteristics in KrF. Figure 1 is a schematic of the measurement system.

A tunable dye laser is pumped by a pulsed Nd:YAG laser tripled to 355 nm. The dye output is then doubled utilizing a BBO crystal cut for 250 nm. Due to gain around 248 nm, the absorption characteristics of the medium must be measured by tuning the probe light sufficiently away from 248 nm to avoid detecting any off-line gain. It is found that the

probe wavelengths must be at least  $\approx 8$  nm on either side of line center to avoid any appreciable gain contributions. The wavelengths chosen for the off-line measurements are 240.0 nm and 257.3 nm. (The absorption on line center is calculated by performing a linear interpolation between the 240.0 nm and 257.3 nm data.)

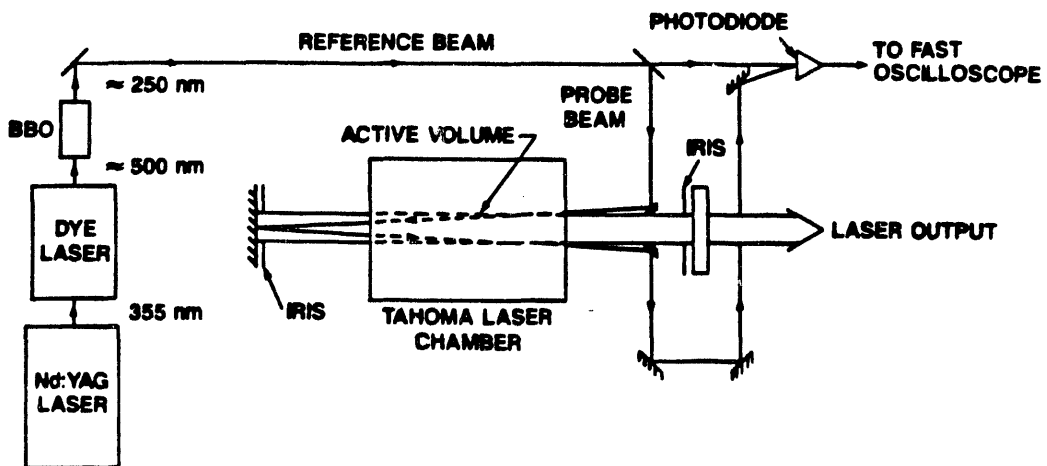


Fig. 1. Schematic of transient absorption measurement system.

A beam splitter divides the primary beam into two beams. The transmitted beam (reference) travels directly to a photodiode while the reflected beam (probe) is directed through an optical delay path that includes two passes through the laser chamber before detection by the same photodiode. Employing a single photodiode eliminates the need to calibrate multiple detectors. The optical delay is long enough to allow viewing both reference and probe signals without temporal overlap. The probe is inserted into and extracted from the oscillator cavity without interfering with the intracavity flux by using small turning prisms. Intracavity irises control the output laser beam diameter to prevent coupling any significant laser radiation into the prisms and the photodiode. Note that the rear high reflector mirror of the laser cavity also serves as the middle mirror for the double pass of the probe beam. Although a convenient method for enabling the double pass of the probe beam, this feature also tends to complicate the analysis of the absorption data because of amplified spontaneous emission (ASE) effects during nonlasing conditions. This will be discussed later. The intracavity flux is varied by simply changing the output couplers.

Additional diagnostics not shown in Figure 1 are two photodiodes and an laser energy meter. One photodiode measures the laser pulse profile by detecting the small amount of laser light that leaks through the high reflector, and the second photodiode detects the sidelight fluorescence at the center of the active volume. The energy meter measures the laser output fluence from which the intracavity flux can be calculated.

The KrF gas mixtures studied are an argon diluent mix (14.5% Kr) and an argon-free (99.8% Kr) mix at total pressures of 1004 and 665 torr, respectively. For both mixtures, the F<sub>2</sub> pressure is kept constant at 2.8 torr.

As mentioned earlier, the feedback from the high reflector during nonlasing conditions aggravates the ASE loading within the cavity. This potentially impacts the absorption measurements because during nonlasing there may still be an appreciable amount of intracavity flux present due to ASE. An ASE code developed at STI<sup>3</sup> predicts 520 kW/cm<sup>2</sup> of flux loading based on the gain measurements made by probing on-line center at 248.4 nm. As will be shown, the saturable loss component  $a_s$  requires  $> 1$  MW/cm<sup>2</sup> to saturate. Consequently, the ASE effects can be considered negligible and are therefore ignored throughout the analysis.

### Results

Figure 2 shows the measured absorption values versus the average intracavity flux. The average flux is calculated using the measured laser output fluences in the aforementioned ASE code. As part of its calculations, the code also calculates the flux conditions during lasing within the cavity. For this data, the pumping rate is  $\approx 386 \text{ kW/cm}^3$ .

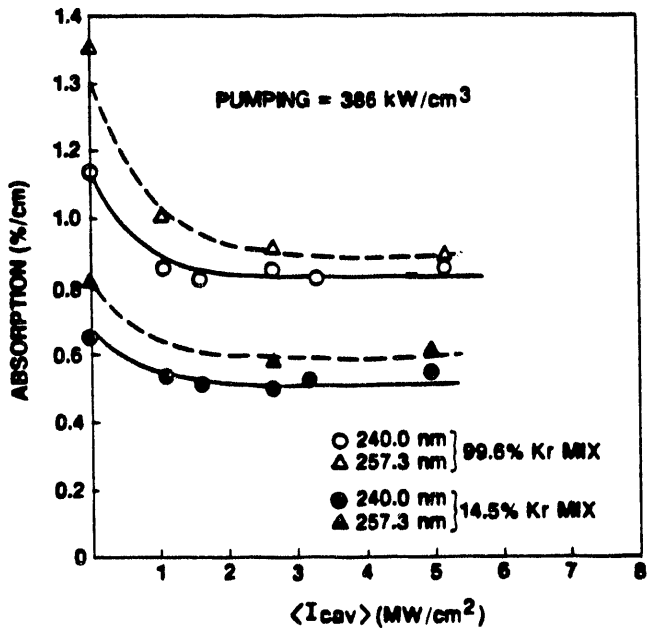


Fig. 2. Absorption data as a function of the average intracavity flux.

The absorption results for both Kr-rich (open symbols) and Ar-diluent mixtures (closed symbols) are presented. The graph shows that at both probe wavelengths, the absorption for the Ar-diluent mix is always smaller at a given flux loading than for the Kr-rich mix. Also, the absorption at 257.3 nm is always higher than at 240.0 nm. The higher absorption at the longer wavelengths has been observed by others and is probably due to absorbing species such as  $\text{Kr}_2\text{F}^+$ ,  $\text{Ar}_2^+$ , and  $\text{Kr}_2^+$ .

With regard to the effects of the intracavity flux, for an average flux of  $\approx 1.5 \text{ MW/cm}^2$ , the absorption in all cases drops to a constant level which is interpreted as representing the nonsaturable loss. Performing the experiment at 15% to 20% higher deposition yields nearly identical results.

### Discussion

The absorption at 248.4 nm, derived by linear interpolation of the 240.0 nm and 257.3 nm absorption data, are summarized as follows. For the Kr-rich mixture, the small signal absorption (saturable + nonsaturable) is  $1.25\%/\text{cm}$ , which is 64% larger than the absorption for the Ar-diluent mixture at  $0.76\%/\text{cm}$ . For the saturable absorption component, it is found that:  $a_s(\text{Kr-rich}) \approx 2.5 a_s(\text{Ar-diluent})$ . While for the nonsaturable component the relationship is:  $a_n(\text{Kr-rich}) \approx 1.5 a_n(\text{Ar-diluent})$ . Finally, the data indicates that saturation of  $a_s$  requires a flux of  $\approx 1.5 \text{ MW/cm}^2$ .

Comparison of the results obtained at STI with other results found in the literature,<sup>2,4-5</sup> show a general tendency for the absorption to increase with deposition rate. Figure 3 shows the measured small signal absorption versus deposition rate. Also plotted is the LANL model prediction of the small signal absorption for pumping rates

<500 kW/cm<sup>3</sup> (10% Kr mixture). The agreement with the data is fair.

Additional work is in progress to consolidate the absorption data with other measurements performed on the laser in order to complete the characterization package for the model validation.

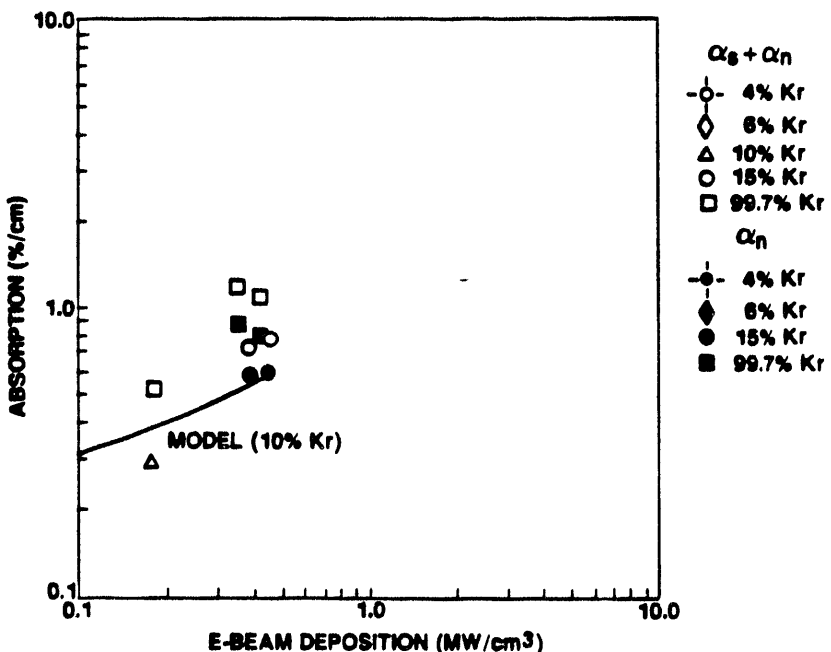


Fig. 3. Absorption data as a function of the e-beam deposition. The solid curve is the prediction from the LANL model for a 10% Kr mixture.

#### Acknowledgments

This work was support by Los Alamos National Laboratory, Contract No. 9-X65-W1478-1.

#### References

1. A.M. Hawryluk, J.A. Mangano, and J.H. Jacob, *Appl. Phys. Lett.* 31, 164 (1977).
2. D.C. Thompson, R. Fedosejevs, and A.A. Offenberger, Conference on Lasers and Electro-optics (CLEO), April 25-29, 1988, Anaheim, CA, Session TUB1.
3. D.D. Lowenthal, Spectra Technology, Inc. (private communication).
4. C.B. Edwards, F. O'Neill, and M.J. Shaw, *Appl. Phys. Lett.* 38, 843, (1981).
5. E.T. Salesky and W.D. Kimura, *Appl. Phys. Lett.* 46, 927, (1985).

#### **DISCLAIMER**

This report was prepared as an account of work sponsored by an agency of the United States Government. Neither the United States Government nor any agency thereof, nor any of their employees, makes any warranty, express or implied, or assumes any legal liability or responsibility for the accuracy, completeness, or usefulness of any information, apparatus, product, or process disclosed, or represents that its use would not infringe privately owned rights. Reference herein to any specific commercial product, process, or service by trade name, trademark, manufacturer, or otherwise does not necessarily constitute or imply its endorsement, recommendation, or favoring by the United States Government or any agency thereof. The views and opinions of authors expressed herein do not necessarily state or reflect those of the United States Government or any agency thereof.

DATA  
DECODE  
10/16/94

DATA  
DECODE  
10/16/94

